An Effective Solvent Theory Connecting the Underlying Mechanisms of Osmolytes and Denaturants for Protein Stability

Apichart Linhananta,* Shirin Hadizadeh, and Steven Samuel Plotkin*
Department of Physics and Astronomy, The University of British Columbia, Vancouver, British Columbia, Canada

ABSTRACT An all-atom Gō model of Trp-cage protein is simulated using discontinuous molecular dynamics in an explicit minimal solvent, using a single, contact-based interaction energy between protein and solvent particles. An effective denaturant or osmolyte solution can be constructed by making the interaction energy attractive or repulsive. A statistical mechanical equivalence is demonstrated between this effective solvent model and models in which proteins are immersed in solutions consisting of water and osmolytes or denaturants. Analysis of these studies yields the following conclusions: 1), Osmolytes impart extra stability to the protein by reducing the entropy of the unfolded state. 2), Unfolded states in the presence of osmolyte are more collapsed than in water. 3), The folding transition in osmolyte solutions tends to be less cooperative than in water, as determined by the ratio of van 't Hoff to calorimetric enthalpy changes. The decrease in cooperativity arises from an increase in native structure in the unfolded state, and thus a lower thermodynamic barrier at the transition midpoint. 4), Weak denaturants were observed to destabilize small proteins not by lowering the unfolded enthalpy, but primarily by swelling the unfolded state and raising its entropy. However, adding a strong denaturant destabilizes proteins enthalpically. 5), The folding transition in denaturant-containing solutions is more cooperative than in water. 6), Transfer to a concentrated osmolyte solution with purely hard-sphere steric repulsion significantly stabilizes the protein, due to excluded volume interactions not present in the canonical Tanford transfer model. 7), Although a solution with hard-sphere interactions adds a solvation barrier to native contacts, the folding is nevertheless less cooperative for reasons 1–3 above, because a hard-sphere solvent acts as a protecting osmolyte.

INTRODUCTION

Osmolytes are intracellular organic molecules that stabilize proteins against unfolding under environmental stresses such as high temperatures, desiccation, or chemical denaturants such as urea (1). The stabilizing property of osmolytes has been shown to correlate with the preferential exclusion of osmolytes from unfolded protein domains, resulting in the preferential accumulation of water (i.e., preferential hydration) near an unfolded protein (2,3). This implies a net repulsive interaction between stabilizing osmolytes and protein, and indeed preferential exclusion has been shown to arise from repulsive interactions between osmolytes and the backbone of proteins (4–6). Repulsive osmolyte-backbone interactions would raise the enthalpy of a protein, and the increase in enthalpy would be larger for the unfolded state due to its larger solvent-exposed backbone area. Consequently the unfolded state would be more destabilized, stabilizing the folded native state.

Another possible stabilization mechanism is the osmolyte-induced loss of protein conformational entropy, with greater entropic loss in the unfolded state, leading to an overall shift in equilibrium toward the native state. The entropy loss mechanism is consistent with experimental works that observed increased compactness in unfolded states of chymotrypsin inhibitor 2 (7), cutinase (8), protein S6 (9), and Rnase S (10) due to osmolytes. This would imply that even if an osmolyte interacted with a protein with the same energetics as water, it would still stabilize the protein for entropic reasons. In Ratnaparkhi and Varadarajan (10), which examines the thermal and chemical stabilization of Rnase S by osmolytes, protein stabilization due to enthalpy increase of the unfolded state is ruled out. Excluded volume effects were also seen to be the primary stabilizing force for yeast iso-1-ferricytochrome *c* in polyol osmolytes (11). Experimental evidence generally supports protein stabilization by loss of protein conformational entropy of the unfolded state in the presence of osmolytes.

In contrast to protecting osmolytes, denaturants such as urea and Guanadinium chloride (GdnHCl) are nonprotecting osmolytes. The interaction between urea or GdnHCl and the protein is attractive, leading to the preferential accumulation of denaturant in the vicinity of proteins (12). The attractive denaturant-protein interactions lower the free energy of both the N and U states, but due to its larger solvent-exposed surface area, the free energy of the U state is lowered more compared to the folded state (5). As in the above case of osmolyte-induced stabilization, another possible mechanism is that the presence of denaturant increases the protein conformational entropy in the unfolded state more so than in the folded state, and this leads to net destabilization. Consequent to either mechanism, the addition of urea to protein solutions shifts the equilibrium to the unfolded state. The attractive interactions between

Submitted February 10, 2010, and accepted for publication November 15, 2010.

*Correspondence: steve@physics.ubc.ca or apichart.linhananta@lakeheadu.ca

Apichart Linhananta's present address is Physics Department, Lakehead University, 955 Oliver Road, Thunder Bay, Ontario, Canada.

Editor: Gerhard Hummer.

0006-3495/11/01/0459/10 $2.00

doi: 10.1016/j.bpj.2010.11.087

urea and protein must overcome excluded volume-driven entropic stabilization of the protein.

There have been relatively few theoretical or computer simulation investigations of proteins in aqueous solution of osmolytes and denaturants. All-atom molecular dynamics (MD) simulations of proteins in aqueous solution of trimethylamine *n*-oxide (TMAO) were used to show that the stabilization property of the osmolyte arises from enhanced water structures (13). All-atom MD simulations have been performed to show that urea destabilizes proteins by direct and water-assisted urea-protein interactions (12,14,15), and denaturation thermodynamics investigated (16). There have also been MD simulations of polymer and small hydrocarbons (17,18) and RNA hairpin (19) immersed in solutions of osmolytes or urea.

A general description of protecting and denaturing (urea) osmolytes has been proposed by Bolen and Rose (5), by developing Tanford's transfer model (20) to account for both protein side chains and backbone. Essentially the same thermodynamic cycle approach has been applied to theories of protein stabilization due to macromolecular crowding agents (21,22), which focus on the excluded volume (entropic) aspects of the transfer process. The similarity in these approaches is no coincidence, as a macromolecular confiner is essentially a stabilizing osmolyte of large effective size. In fact, the physical origins of protein or polymer stabilization by steric osmolytes or crowders are essentially the same as those leading to phase separation in colloidal suspensions due to the addition of a nonadsorbing polymer, for example (23). We hope in this article to unify some of the concepts that have developed in parallel in the fields of osmolytes, crowding, and colloidal systems.

We adopt Bolen's classification of solvents as either "good" or "poor" in comparison to water, even though our solvents may not be good or poor by the more rigorous definition of Flory scaling exponents. In a poor solvent (solvophobic), protein intramolecular interactions dominate, which favors a compact folded native state that minimizes solvent-exposed protein surface area. In a good solvent (solvophilic), protein-solvent interactions dominate, which favors an unfolded state that maximizes protein-solvent contacts. At the middle of the solvent quality scale is the neutral solvent that favors neither native nor unfolded states. Water is a poor solvent for proteins because the effective water-protein interactions lead to the hydrophobic effects, one of the major forces that fold proteins. Aqueous osmolyte solution and aqueous denaturant solution (at high enough concentration) are poor and good solvent, respectively.

The solvent quality paradigm led to several molecular free energy transfer models, which are phenomenological models that utilize as input the experimentally measured change in free energy of proteins on transfer from pure water to aqueous osmolyte/denaturant solutions (24,25). A recent study combined Gō model simulation data with experimentally measured transfer free energies to show that solutions of TMAO and urea raise and lower, respectively, the folding temperatures (26). Although the predicted transfer-enthalpy changes into TMAO/urea utilize experimental data, the transfer model may lead to an incomplete description of the change in protein conformational entropy by not taking into account excluded volume effects, which reduce the number of accessible protein conformations.

MODELS AND METHODS

Discontinuous molecular dynamics (DMD) is an efficient method that has been used to study protein folding (27–30), protein aggregation (31,32), and ab initio protein structure prediction (33). The representative protein used in this work to illustrate the effects of solvent quality is a DMD all-atom model of the Trp-cage protein (16,28,34–37), a designed, 20-residue, truncated construct exhibiting cooperative folding to a stable structure at physiological pH (see Fig. S1 in the Supporting Material). Initial heavy-atom positions were obtained from the NMR structure (structure 1 of PDB 1L2Y (36)) and the missing polar hydrogen molecules are constructed as in Linhananta et al. (28).

As described in the Supporting Material, a Gō model potential (38) is implemented by setting the nonbonded square-well depth ε_{pp} to $-\varepsilon_{Go}$ for all ij pairs in the equilibrated structure with van der Waals (vdW) overlap $r < 1.2\sigma_{ij}^{vdW}$, where σ_{ij}^{vdW} is the sum of the vdW radii $r_i + r_j$ for each atom; for all other nonbonded ij pairs, the square-well depth is set to 0, so that these atom pairs are purely repulsive. The energy scale is set by the Gō contact energy as in previous DMD studies (28,39); thus simulations are performed with the Gō contact energy ε^*_{pp} set to $-\varepsilon_{Go} = -1$, and all energies and temperatures are scaled in units of ε_{Go} ($E^* = E/\varepsilon_{Go}$ and $T^* = k_BT/\varepsilon_{Go}$). More details of the DMD model method are contained in the Supporting Material.

The Gō model protein in explicit solvent is implemented by placing the Trp-cage protein in a 40 Å × 40 Å × 40 Å box, along with a variable number of spherical solvent molecules randomly inserted without hardcore overlaps (see Fig. S1). Standard periodic boundary conditions are implemented. A typical simulation consisted of 1000 spherical solvent particles of radius 1.5 Å (the approximate radius of water). This is approximately one-half the number of water molecules in a 55 M solution for a $(40\ \text{Å})^3$ box. We employ such a dilute concentration for computational convenience; physical concentrations have collision times sufficiently short as to make such simulations prohibitively slow. Diluting the concentration weakens the effects that would be observed by varying solvent qualities from those at 55 M, i.e., this simplification effectively places lower bounds on any trends that we predict would be observed. For this reason we find the approximation acceptable, inasmuch as it only strengthens the conclusions of this study.

Solvent molecules interact with both protein moieties and with each other by a square-well potential with well position given by $0.8\sigma_{ij}^{xs} < r < 1.2\sigma_{ij}^{xs}$ and well-depth given by the parameter ε_{xs} or $\varepsilon_{xs}/\varepsilon_{Go} = \varepsilon^*_{xs}$, where x may be either a protein atom p or another solvent residue s. If $r < 0.8\sigma_{ij}^{xs}$, the potential is ∞. For solvent-solvent interactions, σ_{ij}^{ss} is the vdW diameter of the solvent, which we generally set to $\sigma_{ij}^{ss} = 3.0$ Å: roughly the size of a water molecule. ε^*_{ss} is the solvent-solvent square-well depth in units of the Gō contact energy ε_{Go}. For solvent-protein interactions, $\sigma_{ij}^{ps} = \frac{(\sigma_i^{vdW} + \sigma_j^{water})}{2}$ is the average vdW diameter of the protein-solvent (i,j) pair, where σ_i^{vdW} is the vdW diameter of the i^{th} atom of the protein according to CHARMM potential set 19 (40), and $\sigma_j^{water} = 3.0$ Å is the vdW diameter of the j^{th} water molecule. ε^*_{ps} is the protein-solvent square-well depth in units of the Gō contact energy ε_{Go}. A plot of this potential for several values of protein-solvent interaction energy is shown in Fig. S2.

The quantity ε^*_{ps} is a measure of the solvent quality. As shown below through a correspondence between explicit and implicit solute, it is a well-defined function of solute interactions with the protein. In this study the solvent quality is varied from a minimum value of $\varepsilon^*_{ps} = -0.6$ representing a strongly denaturing aqueous urea solution, to a maximum value

of $\varepsilon^*_{ps} = +0.8$ representing a strongly protein-stabilizing aqueous osmolyte solution. We consider $\varepsilon^*_{ps} = 0$ as representing a reference solution of "pure-water" (this is still stabilizing for the protein because $\varepsilon^*_{ps} = -1$). The solvent-solvent square-well depth is generally taken to be $\varepsilon^*_{ps} = -1.0$, reflecting an overall preference for solvent particles to interact with each other at least as favorably as with the protein ($\varepsilon^*_{ss} < \varepsilon^*_{ps}$).

Free energy, energy, and entropy functionals

Energy, entropy, and free energy surfaces (41,42) as a function of an order parameter Q are constructed using the standard multiple-histogram method (43,44), and used to analyze protein folding thermodynamics. Details of the multiple-histogram construction are given in section S1 *B*. Functionals are in units of the Gō contact energy ε_{GO}.

Native contacts are defined by counting all atom pairs in the native structure that are within 1.2 times the sum of their hard-core radii, and between residues i, j such that $|i-j| > 3$, giving 276 contacts in the native state. The fraction Q of these contacts present in a partly folded configuration varies from 0 to 1.

The correspondence between explicit and implicit osmolyte models

A particular effective solvent system, with one species of solvent particle and characterized by three contact energies $\varepsilon^*_{pp}, \varepsilon^*_{ps}, \varepsilon^*_{ss}$, can be shown to be equivalent (in the sense defined below) to a given solution with explicit solute in solvent, characterized by six parameters, $\varepsilon_{pp}, \varepsilon_{ps}, \varepsilon_{op}, \varepsilon_{oo}, \varepsilon_{os}, \varepsilon_{ss}$.

After tracing over the osmolyte degrees of freedom, the solution now with implicit osmolytes can be thought of as an effective solvent system. The latter effective solvent system is the one used to obtain our simulation results. The former explicit solvent+osmolyte system consists of protein or polymer monomers (p), solvent such as water (s), and osmolyte solute (o). Here the different sizes of species simply correspond to different coordination numbers q_p, q_s, and q_o for each of the species.

Given the six explicit-system parameters, we seek the three implicit-system parameters that would give the same average interaction probabilities for the system. The derivation and general equations relating the two models are given in the Supporting Material. A system with $\varepsilon_{pp}, \varepsilon_{ps}, \varepsilon_{op}, \varepsilon_{ss}, \varepsilon_{os}, \varepsilon_{oo} = -1.1, +0.25, +1.1, -1.25, -0.8, -0.4$ in units of k_BT, with $q_p, q_o, q_s = 8, 6, 4$ and mol fractions $x_p, x_o, x_s = 0.05, 0.2, 0.75$, has effective energy scales $\varepsilon^*_{pp}, \varepsilon^*_{ps}, \varepsilon^*_{ss} = -1, +0.4, -1$, which is a set of parameters that we often use in our simulations to model an osmolytic solution. For any explicit osmolyte-solvent system, there exists an effective solvent model that captures the mean-field thermodynamics of protein contacts in the original system.

RESULTS

Simulations

The Trp-cage Gō model in implicit solvent, where the effects of water are incorporated into the intraprotein interaction energy, can be used as a reference protein system (Fig. 1 *A*). The system is simulated by DMD, with the initial Maxwell-Boltzmann distribution of particles defining the temperature T^*. Temperature is maintained by random collisions with imaginary heat-bath ghost particles (45). The system exhibits two-state behavior as shown by the heat capacity plot of Fig. 1 *A*, which has a single first-order-like phase transition peak. The folding temperature $T^*_f = 4.05$, at the heat capacity maximum, separates the low temperate native state (N) from the high temperature unfolded (U) state. The plot was obtained by equilibrium simulations at temperatures from $T^* = 3.0$ to $T^* = 6.0$. The error bars were obtained by performing five $t^* = 60{,}000$ (scaled time duration) independent runs at each temperature. To improve the accuracy near the folding temperature, where the fluctuation is high, five $t^* = 300{,}000$ runs were performed at $T^* = 3.8$, 4.0, and 4.2, which reduced the size of the error bar near the folding temperature. However, C^*versus T^* plots obtained from the multiple-histogram method vary negligibly with simulation length as long as a lower time limit (for the Trp-cage model $T^* \sim 60{,}000$) is exceeded, thus the results are statistically reliable.

Fig. 1 *B* shows the probability distribution versus energy at the folding temperature $T^*_f = 4.05$. The probability distribution is bimodal, with peaks at the unfolded and folded energy, no detectable specific intermediate state, and attenuated population between folded and unfolded states, indicating a weakly two-state transition. We show below that an effective solvent with osmolyte present increases the folding temperature of the Trp-cage, and decreases the cooperativity of the transition, whereas an effective solvent modeling the presence of denaturant decreases the folding temperature and increases the cooperativity.

A hard-sphere solvent induces a desolvation barrier between native contacts, but decreases folding cooperativity relative to the implicit solvent model

Fig. 1 *B* shows the distribution of energy in the implicit solvent model at the folding temperature (*solid*), as well as distribution of energy of a "reference solvent" model at its own transition midpoint (*dotted*). The reference solvent is self-attractive ($\varepsilon^*_{ss} = -1.0$), but has hard-sphere interactions with the protein ($\varepsilon^*_{ps} = 0$). One can see here that the distribution of energy of the hard-sphere solvent is less cooperative than that of the implicit solvent model. However, the protein in hard-sphere solvent still exhibits solvation barriers for native protein contacts (see Fig. 1 *A*, *inset*). Detailed discussion of solvation effects in the model is given in Fig. S6, Fig. S7, Fig. S8, Fig. S9, and Fig. S10.

Solvation barriers are thought to generally increase folding cooperativity, essentially by reducing the conformational space sampled by the protein in partially unfolded states. However, native-centric modeling alone, where pair potentials are modified to mimic solvation barriers (46,47), neglects other potential effects of the solvent on the unfolded ensemble. One important effect is the reduction of polymer entropy in the unfolded state by induced polymer collapse, which results in an increased propensity for native and nonnative contact formation and reduced cooperativity. Thus, solvation barriers by themselves do not imply increased cooperativity. On the other hand, a denaturing osmolyte such as urea or GdnHCl has attractive interactions with the protein that result in expansion of the unfolded state

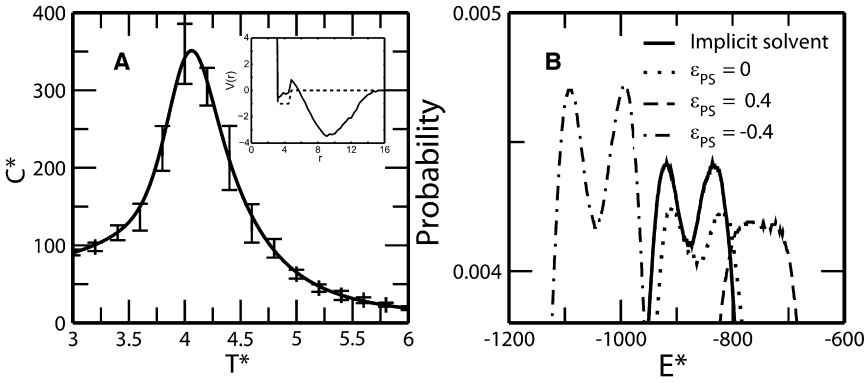

FIGURE 1 (*A*) Reduced heat capacity ($C^* = C_V/k_B$) versus reduced temperature T^* of Trp-cage Gō model with implicit solvent. The plot is obtained by using the multiple-histogram method. The data points and error bars are averages taken from five independent runs at each temperature. (*Inset, dashed curve*) Pair potential for the native contact C(12)-N(46). (*Inset, solid curve*) Transfer PMF superposed on the pair potential in a neutral solvent, obtained by averaging the change in PMF over several native contacts upon transfer to the neutral solvent (see the Supporting Material for further description). (*B*) Probability distributions of energy for protein-protein plus protein-solvent interactions, obtained by the histogram method, for several solvents at their respective folding temperatures (implicit solvent, $T^*_f = 4.05$; neutral solvent with $\varepsilon^*_{ps} = 0$, $T^*_f = 4.55$; protective osmolyte solvent with $\varepsilon^*_{ps} = 0.4$, $T^*_f = 5.08$; and denaturing osmolyte solvent with $\varepsilon^*_{ps} = -0.4$, $T^*_f = 3.91$). For explicit solvents, the energy generally includes protein-solvent interaction energy; however, for the implicit and neutral hard-sphere solvent, this contribution to the energy is zero. Protective osmolytes shift to higher energies and show less cooperative transition, whereas denaturing osmolytes shift to lower energies and show more cooperative transition. Comparing the neutral and implicit solvent histograms, the native ensemble shifts to higher energy because it has less overall native structure due to the less cooperative folding transition. The unfolded ensemble also shifts to the right because even though there is a tendency to have more native long-range contacts (with $|i-j| \geq 4$), there are fewer local contacts.

and increased folding cooperativity, along with solvation barriers. We describe these effects further in Discussion and Conclusions, and in the Supporting Material.

Effects of osmolytes and denaturants on stability, polymer collapse, and folding cooperativity

Fig. 2 *a* shows C^* versus T^* plots of Trp-cage Gō model immersed in 1000 spherical solvent molecules with hard-sphere radius $r_{s,\,hs} = 1.5$ Å (approximately the size of a water molecule) confined in a 40 Å × 40 Å × 40 Å periodic box. For this system the solvent-solvent contact energy is fixed at $\varepsilon^*_{ss} = -1.0$, with the solvent-protein contact energy varying from $\varepsilon^*_{ps} = -0.6$ (strong urealike solution) to $\varepsilon^*_{ps} = 0.8$ (strong osmolyte solution). A plot of the potential function for several values of ε^*_{ps} is shown in Fig. S2. For the neutral solvent ($\varepsilon^*_{ps} = 0$), the folding temperature increases to $T^*_f = 4.5$ and the heat capacity peak has decreased to $C^*_{peak} = 300$, compared to $C^*_{peak} = 350$ for the Trp-cage in implicit solvent (Fig. 1 *A*).

The increase in the folding temperature as compared to the implicit solvent model, despite zero solvent-protein contact energy, suggests that the change in thermodynamic property is due to excluded volume effects. That is, this significant change in stability is due to volume effects not accounted for in the Tanford transfer model (20), which is based upon interactions at the protein-solvent interface and thus has free energies scaling with solvent-accessible surface area, and energy of solvent-protein interaction.

For $\varepsilon^*_{ps} = 0$, there is no energy scale in the problem. For the osmolyte solvents (i.e., poor solvents), in which solvent molecules are repulsive to the protein ($\varepsilon^*_{ps} > 0$), the folding temperature increases progressively to $T^*_f = 5.3$ for $\varepsilon^*_{ps} = 0.8$, and the heat capacity peak also decreases progressively to $C^*_{peak} = 200$ for $\varepsilon^*_{ps} = 0.8$. The addition of repulsive osmolyte solvents (bad solvents) stabilizes the Trp-cage, because the shift of the heat capacity peak indicates the native state is stable up to a higher temperature. For urealike solvents (i.e., good solvents), in which solvent molecules are attracted to the protein ($\varepsilon^*_{ps} < 0$), the folding temperature decreases progressively to $T^*_f = 3.5$, for $\varepsilon^*_{ps} = -0.6$. The attractive urea-solvent interactions destabilize the native structure so that the Trp-cage unfolds at lower temperatures than for the reference (waterlike) solvent with $\varepsilon^*_{ps} = 0$. The set of temperatures T^*_f of heat capacity peaks in Fig. 2 *a* and their corresponding interaction energies ε^*_{ps} define a phase boundary between native (N) and unfolded (U) states. A solvent quality phase diagram can thus be plotted as in Fig. S3.

For each of the solutions plotted in Fig. 2 *a*, the thermal average radius of gyration R_{GY} of the unfolded states with $Q' < 0.2$ was recorded at the corresponding folding temperature; the results are plotted n Fig. 3 *a*. The plot clearly shows that unfolded states become more collapsed as the solvent models one containing osmolyte (i.e., as ε^*_{ps} increases to positive values), and more expanded or swollen as the solvent models one containing denaturant (more negative ε^*_{ps}). Inset images of Fig. 3 *a* show representative snapshots illustrating that unfolded states become more collapsed as solvent quality decreases (as ε^*_{ps} increases). Error bars in the plot are obtained from the standard deviation of the R_{GY} values from simulations of half the total length of those used to obtain the plotted data points. In contrast, folded configurations with $Q > 0.6$ do not show significant variation with solvent quality parameter ε^*_{ps} (data not shown). The trend in Fig. 3 *a* is also consistent with experimental evidence that in the presence of osmolytes, unfolded conformations of proteins become more compact, whereas folded conformations are unaffected (7–10).

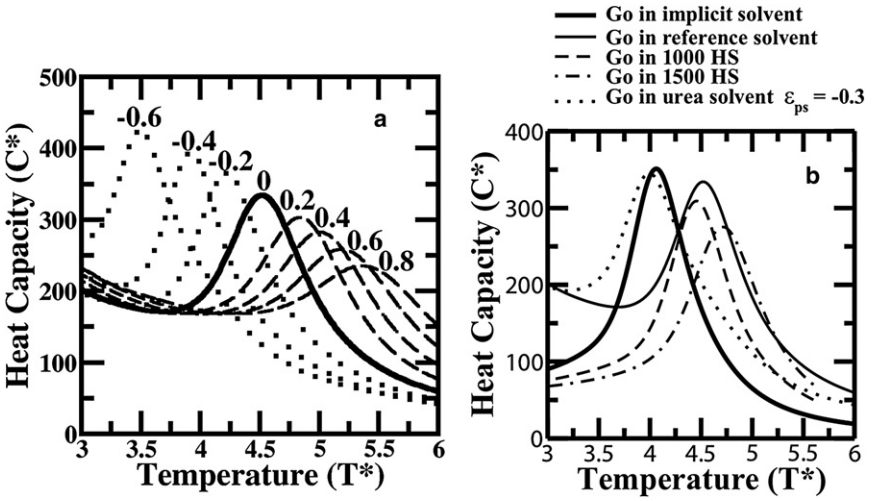

FIGURE 2 (*a*) C^* versus T^* of Trp-cage in solvent for protein-solvent contact energy $\varepsilon^*_{ps} = 0$ (*solid line*); $\varepsilon^*_{ps} = 0.2$, 0.4, 0.6, and 0.8 (*dashed lines*); and $\varepsilon^*_{ps} = -0.2$, -0.4, and -0.6 (*dotted lines*). $\varepsilon^*_{ss} = -1$ for all solvents. (*b*) C^* versus T^* of plots Trp-cage for several solvent models. In implicit solvent (*thick solid line*), in 1000 spherical reference solvent molecules with $\varepsilon^*_{ss} = -1$, $\varepsilon^*_{ps} = 0$ (*thin solid line*, this curve is identical to the $\varepsilon^*_{ps} = 0$ curve in panel *a*); in 1000 pure hard-sphere spherical solvents with $\varepsilon^*_{ss} = 0$, $\varepsilon^*_{ps} = 0$ (*dashed line*); in 1500 pure hard-sphere spherical solvents $\varepsilon^*_{ss} = 0$, $\varepsilon^*_{ps} = 0$ (*dashed-dotted line*); and in 1000 urealike spherical solvents with $\varepsilon^*_{ss} = -1$, $\varepsilon^*_{ps} = -0.3$ (*dotted line*).

We also plot the cooperativity of the transition versus ε^*_{ps} in Fig. 3 *b*. The cooperativity is defined by the ratio of the van't Hoff enthalpy over calorimetric enthalpy, $\Delta H_{vH}/\Delta H_{cal}$, of the folding transition (48–51). We show in Fig. S5 *B* that the internal enthalpy of protein-protein plus protein-solvent interactions is a nearly linear function of Q, hence we use Q here as a proxy for the internal enthalpy of the system, rather than computing the total enthalpy and subtracting baselines. As well, we show in the Supporting Material that fluctuations in Q approximately reproduce the same heat capacity scan as the enthalpy, up to a trivial scaling factor that is irrelevant for the ratios calculated below (see Fig. S4).

The various enthalpies are calculated as follows. The van't Hoff enthalpy change corresponds to twice the standard deviation of the enthalpy (or Q) at the transition midpoint, whereas the calorimetric enthalpy corresponds to the difference in enthalpy of the unfolded and folded states well above and below the transition, respectively (49). We found these values by taking the average values of Q both well below and well above the transition. The corresponding values of Q_f and Q_u did not vary significantly as ε^*_{ps} varied. In contrast, the van't Hoff enthalpy varies significantly, as can be seen from the insets in Fig. 3 *b* which show histograms of Q at the transition midpoints for $\varepsilon^*_{ps} = -0.6$ and $\varepsilon^*_{ps} = +0.8$. Denaturant solutions show enhanced two-state behavior of the transition, with larger cooperativity and corresponding bimodal distribution of Q-values at the transition midpoint. Osmolyte solutions show reduced two-state behavior of the transition, with smaller cooperativity and unimodal (at least for the Trp cage model) distribution of Q-values at the transition midpoint.

Excluded volume stabilization due to hard sphere solvents

Fig. 2 *b* compares the Trp-cage in implicit solvent (*thick solid*) with Trp-cage immersed in 1000 (*dashed*) and 1500 (*dashed-dotted*) pure hard-sphere solvent (HSS) molecules with $\varepsilon^*_{ss} = 0$ and $\varepsilon^*_{ps} = 0$, where the hard-sphere radius of a solvent molecule is 1.2 Å, roughly 80% of the vdW radius of a water molecule (see Models and Methods). The HSS systems differ from the implicit solvent system: The folding temperature increases from $T^*_f = 4.0$ (implicit solvent) to $T^*_f = 4.45$ (1000 HSS) to $T^*_f = 4.7$ (1500 HSS). This is despite the fact that the interactions between the HSS molecules with themselves and with the protein are purely steric, so there is no energy scale in the problem other than temperature. This indicates that protein stabilization is purely due to an excluded volume effect. The addition of explicit solvent molecules reduces the configuration/conformation space of the protein, to different extents depending on whether the protein is folded or unfolded.

Even for weak denaturant solution where the protein is weakly attractive to the protein, such as $\varepsilon^*_{ps} = -0.2$ of Fig. 2 *a*, the folding temperature is higher than that of the Trp-cage implicit solvent model. To compensate for the stabilizing effects of excluded volume, a denaturing solution must have protein-solvent attraction larger than $\varepsilon^*_{ps} = -0.3$ (when $\varepsilon^*_{ss} = -1$), as depicted by the dotted line in Fig. 2 *b*, which has the same folding temperature as the implicit-solvent model $T^*_f = 4.0$, and similar height of the heat capacity peak. This indicates that there is a critical net attractive energy between solute and protein for the solute to function as a denaturant.

Another observation that can be made from Fig. 2 *b* is that the 1000 neutral solvent molecules model (the "reference" solvent with $\varepsilon^*_{ps} = 0$ and $\varepsilon^*_{ss} = -1$) has a folding temperature of $T^*_f = 4.57$ (*light solid line*), which is slightly higher than the 1000 HSS model, suggesting that the attractive solvent-solvent interactions enhance protein stabilization (but to a lesser degree than the excluded volume contribution). This can be thought of as a minimal model of the hydrophobic effect.

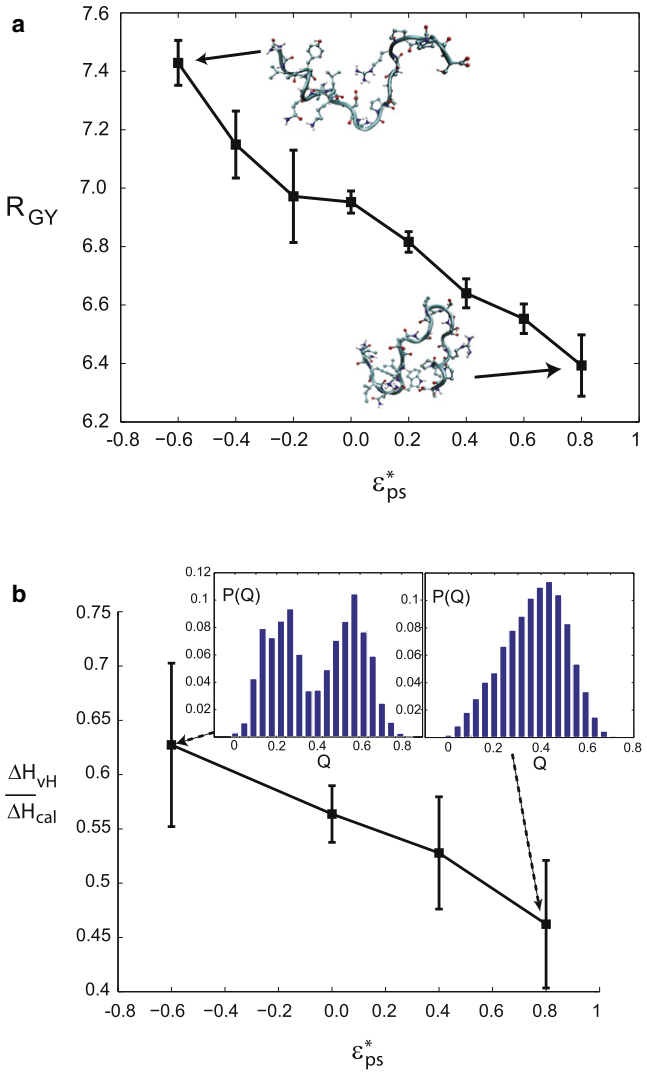

FIGURE 3 (*a*) Radius of gyration of the unfolded states with $Q < 0.2$ taken at the temperatures of the heat capacity peaks in Fig. 2, plotted as a function of the protein-solvent interaction energy ε^*_{ps}. The unfolded states progressively become more collapsed as the solvent moves from that containing denaturant to one containing osmolyte. (*Insets*) Snapshots of representative unfolded states for $\varepsilon^*_{ps} = -0.6$ and $\varepsilon^*_{ps} = +0.8$. These snapshots are obtained by taking the first sampled conformation that had a R_{GY} within 2% of the average value given by the plotted data point. (*b*) Cooperativity of the folding transition, defined by the ratio of the van' t Hoff enthalpy over calorimetric enthalpy, as a function of ε^*_{ps}. The transition becomes more cooperative for denaturant-containing solvents, and less cooperative for osmolyte-containing solvents. (*Insets*) Histograms of the values of Q at the midpoints of the transition (at the respective heat capacity peak temperatures) for $\varepsilon^*_{ps} = -0.6$ and $\varepsilon^*_{ps} = +0.8$, which are strongly bimodal for a denaturant-containing solvent, and unimodal (for the Trp cage model) for a strong osmolyte-containing solvent.

Calculation of the free energy, enthalpy, and entropy changes for osmolytes and denaturants

To understand the mechanism of protein stabilization by osmolytelike solvents, we analyzed structural data to obtain internal free-energy, enthalpy, and entropy as functions of Q, for the protein in solvent models with $\varepsilon^*_{ps} = 0$, 0.4, and -0.2, at a fixed temperature of $T^*_f = 4.8$. At this temperature, the neutral solvent ($\varepsilon^*_{ps} = 0$, $T^*_f = 4.57$) and the weakly urealike model ($\varepsilon^*_{ps} = -0.2$, $T^*_f = 4.24$) are in the unfolded (U) state, whereas the osmolytelike model ($\varepsilon^*_{ps} = 0.4$, $T^*_f = 5.0$) is in the native (N) state. Fig. 4 *a* plots the free energy versus Q at $T^*_f = 4.8$ for the three solvents models. For the neutral solvent ($\varepsilon^*_{ps} = 0$), the U state is stable as evident from the minima at $Q_{min} \sim 0.1$. The osmolyte solvent ($\varepsilon^*_{ps} = 0.4$) stabilizes the protein so that the free energy minima is now at $Q_{min} \sim 0.5$, indicating a stable N state. The osmolytic solvent with $\varepsilon^*_{ps} = 0.4$ stabilized the native state by $\approx 5\ k_BT$. The relatively low value $Q_{min} \sim 0.5$ is because the folding temperature of the protein-osmolyte system ($\varepsilon^*_{ps} = 0.4$) is $T^*_f = 5.0$ (Fig. 2 *a*), which is only slightly higher than $T^* = 4.8$, and also because a protein of such small size as the Trp cage exhibits substantial fluctuations in the native basin. In the case of denaturing solvents ($\varepsilon^*_{ps} = -0.2$), the protein is even more destabilized than the neutral solvent with a further change of stability of $\sim -4\ k_BT$, and a shift of the free energy toward lower Q values in Fig. 4 *a*.

Fig. 4 *b* plots the total thermal energy $\langle E \rangle$ (protein-protein + protein-solvent + solvent-solvent energy) versus Q at $T^* = 4.8$ for $\varepsilon^*_{ps} = 0$, 0.4, and -0.2, and Fig. 4 *d* plots the differences (upon transfer) relative to the $\varepsilon^*_{ps} = 0$ model. Fig. 4 *d* readily shows that the osmolyte ($\varepsilon^*_{ps} = 0.4$) solvent lowers the energy of the protein uniformly (even though the solvent-protein interaction is repulsive). An osmolytic solvent with repulsive ε^*_{ps} lowers the energy by inducing collapse in the protein in a manner that for 1L2Y is not sensitive to Q over the range spanning the unfolded and folded states. Hence the stabilization of protein in our model is not enthalpically driven, because the osmolyte solvents decrease the energy of the native (high Q) and unfolded (low Q) essentially equally. Denaturant-containing solvents ($\varepsilon^*_{ps} = -0.2$) raise the internal energy of the unfolded state relative to neutral solvent (even though the solvent-protein interaction is attractive) rather than lowering it. This is due to the fact that as favorable solvent-protein contacts are made, favorable protein-protein contacts are lost, so that the net result is a modest stabilization of the native state change due to enthalpy changes (see Fig. 4 *d* and compare to Fig. S5).

Fig. 4 *c* plots the entropy S versus Q, which shows a decrease/increase in the entropy of the unfolded protein for the osmolyte/denaturant solution, compared to the neutral solvent. The entropy difference between osmolyte/denaturant solvents and neutral solvent (i.e., upon transfer) is plotted in Fig. 4 *e*. For the osmolyte solvents ($\varepsilon^*_{ps} = 0.4$), the decrease in entropy relative to the neutral solvent is due to the excluded volume effects, which are expected to reduce the protein conformational/spatial configurations. The key point is that the reduction in entropy becomes more significant as Q decreases (see *dashed line* of Fig. 4 *e*), which means that the entropy of unfolded conformations is reduced more

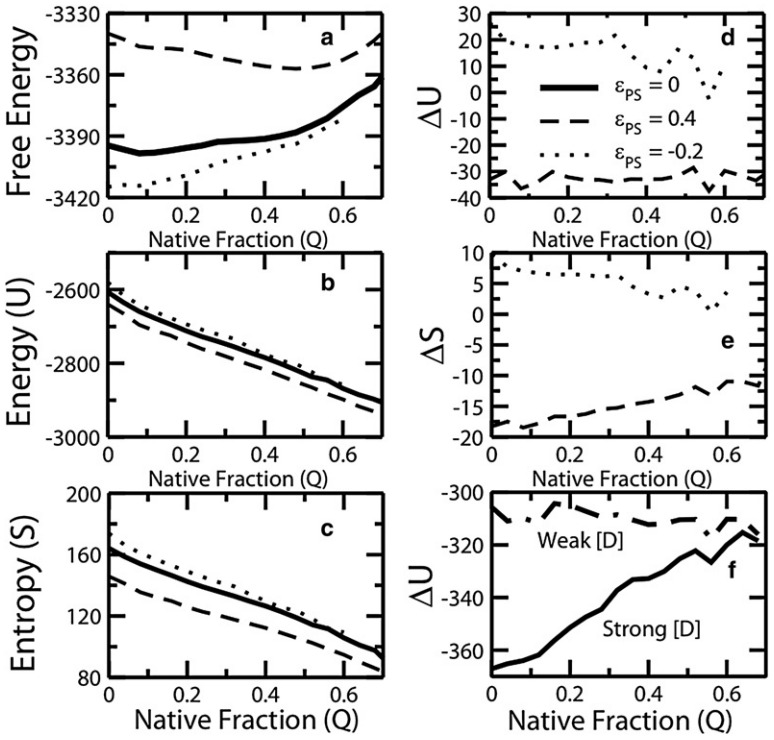

FIGURE 4 (*a*) Free energy versus protein native fraction (Q) at $T^* = 4.8$ for $\varepsilon^*_{ps} = 0$ (*solid line*), $\varepsilon^*_{ps} = 0.4$ (*dashed line*), and $\varepsilon^*_{ps} = -0.2$ (*dotted line*), with solvent-solvent contact energy fixed at $\varepsilon^*_{ss} = -1$. (*b*) Total energy $\langle E \rangle$ versus Q. (*c*) Entropy (S) versus Q. (*d*) Changes in enthalpy between osmolyte and neutral solvent $\Delta E = E(\varepsilon^*_{ps} = 0.4) - E\ (\varepsilon^*_{ps} = 0)$ (*dashed line*), and between denaturant solvent and neutral solvent $\Delta E = E(\varepsilon^*_{ps} = -0.2) - E\ (\varepsilon^*_{ps} = 0)$ (*dotted line*). (*e*) Change in entropy (ΔS) versus Q, for osmolyte solvent ($\varepsilon^*_{ps} = 0.4$) compared to neutral solvent ($\varepsilon^*_{ps} = 0$), i.e., $\Delta S = S(\varepsilon^*_{ps} = 0.4) - S\ (\varepsilon^*_{ps} = 0)$ (*dashed line*), and for denaturant ($\varepsilon^*_{ps} = -0.2$) solvent compared to neutral ($\varepsilon^*_{ps} = 0$) solvent $\Delta S = S\ (\varepsilon^*_{ps} = -0.2) - S\ (\varepsilon^*_{ps} = 0)$. (*f*) Comparison between weak and strong denaturants, by plotting $E(\varepsilon^*_{ps} = -0.2) - E\ (\varepsilon^*_{ps} = 0)$ (*dash-dotted*, and shifted by -270ε to appear on the same scale) and $E(\varepsilon^*_{ps} = -0.6) - E\ (\varepsilon^*_{ps} = 0)$ (*solid*) versus Q. Strong denaturants enthalpically stabilize the unfolded state relative to the folded state, whereas weak denaturants mildly stabilize the folded state (but entropically destabilize it).

than that of folded conformations. This is consistent with the hypothesis that osmolytes stabilize proteins by introducing an entropic penalty for unfolded conformations.

For denaturant-containing solvents ($\varepsilon^*_{ps} = -0.2$), the increase in entropy relative to the neutral solvent becomes more significant as Q decreases (*dotted line* of Fig. 4 *e*), which means that the entropy of unfolded conformations is increased more than folded conformations. This effect dominates the enthalpic stabilization. These results suggests that urea or GdHCl destabilization of a protein may also be driven by entropy change, at least for weak solutions. The dominant factor contributing to the destabilization of the native state for weak denaturing solvents is the increase in entropy due to expansion of the unfolded state. Swelling of the unfolded state with increasing denaturant concentration has been observed for several proteins (52,53). The above results are also confirmed by investigating the "internal" energy and entropy of the protein, by including only protein-protein and protein-solvent energy (see Fig. S5).

For sufficiently strong denaturants (ε^*_{ps} large and negative) we expect a crossover to a regime where enthalpic stabilization of the unfolded state also becomes significant. This is observed in Fig. 4 *f*: for strong/weak denaturing solutions ($\varepsilon^*_{ps} = -0.6/\varepsilon^*_{ps} = -0.2$), the unfolded state is enthalpically stabilized or weakly destabilized, respectively, upon transfer from neutral solvent. All enthalpies in Fig. 4 *f* are taken at their respective transition temperatures, where sampling for a wide range of Q can be obtained. The data for $\varepsilon^*_{ps} = -0.2$ at temperature $T^* = 4.2$ is remarkably similar to the osmolyte data with $\varepsilon^*_{ps} = +0.4$ in Fig. 4 *d* at temperature $T^* = 4.8$, exemplifying the dual roles of solute interaction strength and temperature.

DISCUSSION AND CONCLUSIONS

In this work we constructed an all-atom Gō model Trp-cage protein (PDB 1L2Y) immersed in explicit solvent molecules to investigate by discontinuous molecular dynamics (DMD) how osmolyte or denaturant stabilizes or destabilizes proteins. The Trp-cage DMD model was immersed in spherical solvent molecules, in which binding of solvent to protein is controlled by a solvent-protein contact energy ε^*_{ps}. Protein stabilization or destabilization in the solvent model used here arises from a change in solvent-protein interactions ε^*_{ps} implicitly accounting for the presence of osmolyte or denaturant.

The interaction parameters of the effective solvent model used in our simulations were shown to be derivable from a system containing explicit osmolyte/denaturant solute in aqueous solvent, by statistical mechanical equivalence of the interaction probabilities within the quasichemical approximation. A system with explicit osmolytes is equivalent to another system with implicit osmolytes but with a different effective solvent-protein interaction strength.

For an aqueous denaturant (a solvent with $\varepsilon^*_{ps} < 0$), the model is in the spirit of an indirect denaturing mechanism (12), but our interpretation is that the resulting indirect mechanism arises as a net effect of direct urea-protein interactions (15,18). In this work, the main objective was to investigate the general and essential thermodynamic features of how

osmolytes or denaturants stabilize or destabilize a protein. We thus did not focus here on the microscopic details of how osmolyte or denaturant interacts with protein backbone or side chains, nor did we treat any additional effects such as those due to angle-dependent hydrogen-bond networks in water. Nevertheless, we believe that a minimal solvent model with implicit solute still addresses many of the fundamental aspects of protein stabilization and destabilization due to osmolytes and denaturants.

The microscopic variable ε^*_{ps} is a control parameter for the solvent quality. Negative or positive values of ε^*_{ps} correspond to better or worse solvents. On transferring the Gō model to a neutral, hard-sphere-like solvent with $\varepsilon^*_{ps} = 0$, there is an increase in folding temperature from the implicit solvent model, and a decrease in cooperativity. This stabilizing effect is due to excluded volume terms not present in the putative Tanford transfer model. The presence of sterically repulsive osmolytes reduces the allowed conformations of a polymer or protein. This is true whether the osmolytes are small or large. Conversely, the presence of a collapsed unfolded state increases the number of configurations of osmolyte compared to the osmolyte entropy of an expanded unfolded state. For a protein in neutral or hard-sphere solvents, native contacts show solvation barriers, despite a decrease in folding cooperativity—i.e., the presence of solvation barriers does not always indicate an increase in cooperativity.

As the solvent quality scale ε^*_{ps} is increased to mimic aqueous osmolyte solutions ("bad" solvents), there is a further increase in folding temperature, a collapse of the unfolded state, and a corresponding loss in cooperativity. The increase in folding temperature with increased ε^*_{ps} demonstrates an osmolyte's ability to protect proteins against thermal or chemical denaturation. The decrease in cooperativity with increasing ε^*_{ps} was observed by an approximant to the ratio of the van't Hoff/calorimetric enthalpy in the model, which results in an increasing width of the unfolding heat capacity peak versus temperature. The decrease in cooperativity correlates with a loss in unfolded conformational entropy of the model protein. This observation agrees with several experimental studies that invoked loss of protein entropy as a mechanism for protein stabilization by osmolytes (8–11).

In contrast, as ε^*_{ps} decreases to negative values, the folding temperature decreases, indicating a destabilization due to the attractive solvent-protein interactions modeling denaturant in solution. Perhaps surprisingly, for weak denaturants the destabilization upon transfer from a waterlike solvent is not enthalpic. That is, upon addition of denaturant, the unfolded enthalpy does not decrease even though the protein-effective solvent interactions are more attractive, but modestly increases because intraprotein interactions in the unfolded state are lost as the protein is swollen in the unfolded state. This results in a net modest enthalpic stabilization of the folded state.

The process of denaturant-induced swelling increases the entropy of the unfolded state, and increases the cooperativity of the folding transition. Thus protein destabilization, due at least to weak denaturants compared to an energetically neutral solvent, is entropic in origin. However, sufficiently strong denaturants were observed to enthalpically stabilize the unfolded protein. We note that we are referring here to relative stabilizing and destabilizing effects upon addition of osmolyte or denaturant to a neutral solvent, not total overall stabilities.

The above crossover results were not observed in an all-atom simulation study of Trp-cage protein in urea (16), which showed a monotonically decreasing enthalpy of unfolding, and an entropic contribution to unfolding that was remarkably independent of urea concentration (to within a fraction of a kJ/mol) over an 8 M range. We believe the reason for this is that in these authors' approach, the enthalpic and entropic parameters were obtained by fitting their data to a Hawley model free energy surface (54), which by construction limited the denaturant-dependence of the energy and entropy of unfolding to be linear, so that nonmonotonic denaturant dependence could not be observed a priori. The results of our model would indicate that a direct computation of the unfolding enthalpy and entropy of unfolding should show the nonmonotonic denaturant dependence that we observed. Investigation of the crossover from entropic to enthalpic dominance of the unfolding mechanism is an interesting topic of future work.

Osmolytes reduce the entropy of the unfolded state by collapsing it, whereas denaturants increase it by expanding it. There is little change in the density or conformational entropy of the folded state, so there is little effect at high degrees of nativeness. The observed trend in cooperativity emerges as a natural consequence of this swelling/collapse. It should be mentioned that this trend is opposite to that observed recently by O'Brien et al. (26) for a coarse-grained model of cold shock protein. These researchers used coarse-grained model proteins in implicit solvent, modeling the effects of osmolyte or denaturant with free energetic parameters taken from the transfer model, and then reweighting the Boltzmann sampling probabilities of simulations that were performed in the absence of solute. They also observed almost no cooperativity trend for their model of protein L. It may be that different proteins have different cooperativity behavior due potentially to different folding mechanisms, e.g., the degree to which collapse occurs concomitantly with folding. Another potential origin of the discrepancy is the explicit accounting of solute-excluded volume effects in our model, which, as we have mentioned, is not present in the putative Tanford transfer model.

We note that an effective solvent model cannot directly capture phenomena such as the preferential exclusion of osmolytes from the vicinity of the protein (2), nor the surfactantlike action of denaturants in weakening hydrophobic interactions (18). Moreover, the coarse-grained solvent in

our model acts similarly on protein amino acids whether polar or hydrophobic, so it is unlikely to be a useful model for understanding phenomena such as cold denaturation or pressure denaturation. On the other hand, an extension of the model could address the effects of differential attraction/repulsion of, say, osmolytes to protein side chains and backbone, by allowing the parameter ε^*_{ps} to vary—depending on which parts of specific amino acids the solutes might happen to interact with.

Here we chose instead to model the averaged effects of osmolytes using a single parameter. The demonstration that the backbone of every amino acid is repulsive to osmolyte regardless of amino-acid type (6) supports the use of an averaged net interaction between osmolytes and amino acids as an acceptable first approximation to address the overall effects of stabilization.

Another future improvement on the model that addresses these issues is the development of models with osmolytes explicitly accounted for. This is a straightforward extension of our model by including two solvent particle species (water and osmolyte) with different sizes and interaction energies. Such an extension allows for the investigation of several new phenomena including preferential exclusion or attraction, explicit concentration dependence, and size dependence, as well as the statistical mechanics of the compensatory mechanisms of osmolytes and denaturants simultaneously present. Exploration of these interesting topics is reserved for a sequel to this article.

SUPPORTING MATERIAL

Model and method, phase diagram, heat capacity and cooperativity analysis, free energy surfaces, formal equivalence between implicit and explicit osmolyte models, and analysis of solvation barriers are available at http://www.biophysj.org/biophysj/supplemental/S0006-3495(10)05212-4.

We acknowledge the use of the Shared Hierarchical Academic Research Computing Network (SHARCNET) for simulations and analysis.

A.L. acknowledges support from the Natural Sciences and Engineering Research Council of Canada, and the Pacific Institute of Theoretical Physics and the University of British Columbia for providing research support during a sabbatical visit when this project was initiated. S.S.P. acknowledges support from the Canada Research Chairs program, the A.P. Sloan Foundation, and the Natural Sciences and Engineering Research Council of Canada.

REFERENCES

1. Yancey, P. H., M. E. Clark, …, G. N. Somero. 1982. Living with water stress: evolution of osmolyte systems. *Science.* 217:1214–1222.
2. Xie, G. F., and S. N. Timasheff. 1997. The thermodynamic mechanism of protein stabilization by trehalose. *Biophys. Chem.* 64:25–43.
3. Xie, G. F., and S. N. Timasheff. 1997. Mechanism of the stabilization of ribonuclease A by sorbitol: preferential hydration is greater for the denatured then for the native protein. *Protein Sci.* 6:211–221.
4. Bolen, D. W., and L. V. Baskakov. 2001. The osmophobic effect: natural selection of a thermodynamic force in protein folding. *J. Mol. Biol.* 310:955–963.
5. Bolen, D. W., and G. D. Rose. 2008. Structure and energetics of the hydrogen-bonded backbone in protein folding. *Annu. Rev. Biochem.* 77:339–362.
6. Auton, M., and D. W. Bolen. 2005. Predicting the energetics of osmolyte-induced protein folding/unfolding. *Proc. Natl. Acad. Sci. USA.* 102:15065–15068.
7. Silow, M., and M. Oliveberg. 2003. High concentrations of viscogens decrease the protein folding rate constant by prematurely collapsing the coil. *J. Mol. Biol.* 326:263–271.
8. Baptista, R. P., S. Pedersen, …, E. P. Melo. 2008. Thermodynamics and mechanism of cutinase stabilization by trehalose. *Biopolymers.* 89:538–547.
9. Chen, L., G. J. Cabrita, …, E. P. Melo. 2005. Stabilization of the ribosomal protein S6 by trehalose is counterbalanced by the formation of a putative off-pathway species. *J. Mol. Biol.* 351:402–416.
10. Ratnaparkhi, G. S., and R. Varadarajan. 2001. Osmolytes stabilize ribonuclease S by stabilizing its fragments S protein and S peptide to compact folding-competent states. *J. Biol. Chem.* 276:28789–28798.
11. Saunders, A. J., P. R. Davis-Searles, …, D. A. Erie. 2000. Osmolyte-induced changes in protein conformational equilibria. *Biopolymers.* 53:293–307.
12. Bennion, B. J., and V. Daggett. 2003. The molecular basis for the chemical denaturation of proteins by urea. *Proc. Natl. Acad. Sci. USA.* 100:5142–5147.
13. Zou, Q., B. J. Bennion, …, K. P. Murphy. 2002. The molecular mechanism of stabilization of proteins by TMAO and its ability to counteract the effects of urea. *J. Am. Chem. Soc.* 124:1192–1202.
14. Klimov, D. K., J. E. Straub, and D. Thirumalai. 2004. Aqueous urea solution destabilizes Aβ(16–22) oligomers. *Proc. Natl. Acad. Sci. USA.* 101:14760–14765.
15. Hua, L., R. Zhou, …, B. J. Berne. 2008. Urea denaturation by stronger dispersion interactions with proteins than water implies a 2-stage unfolding. *Proc. Natl. Acad. Sci. USA.* 105:16928–16933.
16. Canchi, D. R., D. Paschek, and A. E. García. 2010. Equilibrium study of protein denaturation by urea. *J. Am. Chem. Soc.* 132:2338–2344.
17. Athawale, M. V., J. S. Dordick, and S. Garde. 2005. Osmolyte trimethylamine-*n*-oxide does not affect the strength of hydrophobic interactions: origin of osmolyte compatibility. *Biophys. J.* 89:858–866.
18. Zangi, R., R. H. Zhou, and B. J. Berne. 2009. Urea's action on hydrophobic interactions. *J. Am. Chem. Soc.* 131:1535–1541.
19. Pincus, D. L., C. Hyeon, and D. Thirumalai. 2008. Effects of trimethylamine-*n*-oxide (TMAO) and crowding agents on the stability of RNA hairpins. *J. Am. Chem. Soc.* 130:7364–7372.
20. Tanford, C. 1964. Isothermal unfolding of globular proteins in aqueous urea solutions. *J. Am. Chem. Soc.* 86:2050–2059.
21. Zhou, H. X., G. N. Rivas, and A. P. Minton. 2008. Macromolecular crowding and confinement: biochemical, biophysical, and potential physiological consequences. *Annu. Rev. Biophys.* 37:375–397.
22. Zhou, H. X. 2008. Effect of mixed macromolecular crowding agents on protein folding. *Proteins.* 72:1109–1113.
23. Lekkerkerker, H. N. W., W. C. K. Poon, …, P. B. Warren. 1992. Phase-behavior of colloid plus polymer mixtures. *Europhys. Lett.* 20:559–564.
24. Street, T. O., D. W. Bolen, and G. D. Rose. 2006. A molecular mechanism for osmolyte-induced protein stability. *Proc. Natl. Acad. Sci. USA.* 103:13997–14002.
25. Rösgen, J., B. M. Pettitt, and D. W. Bolen. 2005. Protein folding, stability, and solvation structure in osmolyte solutions. *Biophys. J.* 89:2988–2997.
26. O'Brien, E. P., G. Ziv, …, D. Thirumalai. 2008. Effects of denaturants and osmolytes on proteins are accurately predicted by the molecular transfer model. *Proc. Natl. Acad. Sci. USA.* 105:13403–13408.
27. Zhou, Y. Q., and M. Karplus. 1999. Folding of a model three-helix bundle protein: a thermodynamic and kinetic analysis. *J. Mol. Biol.* 293:917–951.

28. Linhananta, A., J. Boer, and I. MacKay. 2005. The equilibrium properties and folding kinetics of an all-atom Gō model of the Trp-cage. *J. Chem. Phys.* 122:1–7.

29. Zhou, Y. Q., C. Zhang, …, J. Wang. 2003. Temperature dependence of the distribution of the first passage time: results from discontinuous molecular dynamics simulations of an all-atom model of the second β-hairpin fragment of protein G. *J. Am. Chem. Soc.* 125:6300–6305.

30. Borreguero, J. M., N. V. Dokholyan, …, H. E. Stanley. 2002. Thermodynamics and folding kinetics analysis of the SH3 domain form discrete molecular dynamics. *J. Mol. Biol.* 318:863–876.

31. Jang, H. B., C. K. Hall, and Y. Q. Zhou. 2004. Assembly and kinetic folding pathways of a tetrameric β-sheet complex: molecular dynamics simulations on simplified off-lattice protein models. *Biophys. J.* 86:31–49.

32. Ding, F., J. J. LaRocque, and N. V. Dokholyan. 2005. Direct observation of protein folding, aggregation, and a prion-like conformational conversion. *J. Biol. Chem.* 280:40235–40240.

33. Ding, F., D. Tsao, …, N. V. Dokholyan. 2008. Ab initio folding of proteins with all-atom discrete molecular dynamics. *Structure.* 16:1010–1018.

34. Huang, X. H., M. Hagen, …, B. J. Berne. 2007. Replica exchange with solute tempering: efficiency in large scale systems. *J. Phys. Chem. B.* 111:5405–5410.

35. Wafer, L. N. R., W. W. Streicher, and G. I. Makhatadze. 2010. Thermodynamics of the Trp-cage miniprotein unfolding in urea. *Proteins.* 78:1376–1381.

36. Neidigh, J. W., R. M. Fesinmeyer, and N. H. Andersen. 2002. Designing a 20-residue protein. *Nat. Struct. Biol.* 9:425–430.

37. Simmerling, C., B. Strockbine, and A. E. Roitberg. 2002. All-atom structure prediction and folding simulations of a stable protein. *J. Am. Chem. Soc.* 124:11258–11259.

38. Gō, N. 1983. Theoretical studies of protein folding. *Annu. Rev. Biophys. Bioeng.* 12:183–210.

39. Zhou, Y. Q., and A. Linhananta. 2002. Role of hydrophilic and hydrophobic contacts in folding of the second β-hairpin fragment of protein G: molecular dynamics simulation studies of an all-atom model. *Proteins.* 47:154–162.

40. Neria, E., S. Fischer, and M. Karplus. 1996. Simulation of activation free energies in molecular systems. *J. Chem. Phys.* 105:1902–1921.

41. Plotkin, S. S., J. Wang, and P. G. Wolynes. 1997. Statistical mechanics of a correlated energy landscape model for protein folding funnels. *J. Chem. Phys.* 106:2932–2948.

42. Plotkin, S. S., and J. N. Onuchic. 2002. Understanding protein folding with energy landscape theory. Part II: Quantitative aspects. *Q. Rev. Biophys.* 35:205–286.

43. Kumar, S., D. Bouzida, …, J. M. Rosenberg. 1992. The weighted histogram analysis method for free-energy calculations on biomolecules. 1. The method. *J. Comput. Chem.* 13:1011–1021.

44. Socci, N. D., and J. N. Onuchic. 1995. Kinetic and thermodynamic analysis of proteinlike heteropolymers—Monte-Carlo histogram technique. *J. Chem. Phys.* 103:4732–4744.

45. Zhou, Y. Q., M. Karplus, …, C. K. Hall. 1997. Equilibrium thermodynamics of homopolymers and clusters: molecular dynamics and Monte Carlo simulations of systems with square-well interactions. *J. Chem. Phys.* 107:10691–10708.

46. Cheung, M. S., A. E. García, and J. N. Onuchic. 2002. Protein folding mediated by solvation: water expulsion and formation of the hydrophobic core occur after the structural collapse. *Proc. Natl. Acad. Sci. USA.* 99:685–690.

47. Ferguson, A., Z. R. Liu, and H. S. Chan. 2009. Desolvation barrier effects are a likely contributor to the remarkable diversity in the folding rates of small proteins. *J. Mol. Biol.* 389:619–636.

48. Zhou, Y. Q., C. K. Hall, and M. Karplus. 1999. The calorimetric criterion for a two-state process revisited. *Protein Sci.* 8:1064–1074.

49. Kaya, H., and H. S. Chan. 2000. Polymer principles of protein calorimetric two-state cooperativity. *Proteins.* 40:637–661.

50. Tanford, C. 1968. Protein denaturation. *Adv. Protein Chem.* 23: 121–282.

51. Privalov, P. L. 1979. Stability of proteins: small globular proteins. *Adv. Protein Chem.* 33:167–241.

52. Schuler, B., and W. A. Eaton. 2008. Protein folding studied by single-molecule FRET. *Curr. Opin. Struct. Biol.* 18:16–26.

53. Ziv, G., and G. Haran. 2009. Protein folding, protein collapse, and Tanford's transfer model: Lessons from single-molecule FRET. *J. Am. Chem. Soc.* 131:2942–2947.

54. Hawley, S. A. 1971. Reversible pressure—temperature denaturation of chymotrypsinogen. *Biochemistry.* 10:2436–2442.